Suppression of Geminate Charge Recombination in Organic Photovoltaic Devices with a Cascaded Energy Heterojunction

Chris Groves

School of Engineering and Computing Sciences, Durham University, South Road, Durham, DH1 3LE, United Kingdom.

e-mail: chris.groves@durham.ac.uk

TABLE OF CONTENTS ENTRY

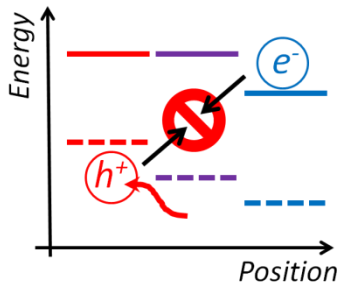

A Monte Carlo model is used to investigate the influence of cascaded energy heterojunctions upon geminate charge recombination within organic photovoltaic devices.

BROADER CONTEXT

The ability to design high-performance organic photovoltaic devices would make it possible to capitalize on their ease of manufacture, and so provide an abundant, cheap, and scalable source of renewable energy. High performance for an organic photovoltaic device requires that charges generated from the absorption of photons must efficiently avoid recombination. One method to achieve this is to utilize an energy cascade encourages the separation of the electron hole pair, similar to photosynthesis. This can be implemented in organic photovoltaics through ternary blends, or in binary blends where one component crystallizes. In this article, the efficacy of this photosynthesis-like process in suppressing geminate charge recombination is examined using a Monte Carlo charge transport model. It is found that cascades can indeed have substantial benefit on device performance but that the degree of benefit depends strongly upon the geometry of the cascade.

ABSTRACT

The effect of cascaded energy heterojunctions on geminate charge recombination in organic photovoltaic devices is examined using a kinetic Monte Carlo model. The structure of the cascaded heterojunction, which encourages spatial separation of the geminate charge pair, is varied to recreate that found in ternary blends and tri-layers, as well as that formed by self-organization in binary blends in which one component crystallizes. It is shown that substantial reductions in charge recombination can indeed be achieved with parameters similar that reported for P3HT:PCBM solar cells. However, the efficacy of cascaded energy heterojunctions is shown to be limited for thick cascade layers (>10nm). This provides guidance as how to design ternary organic photovoltaics, whilst also offering a possible explanation of low recombination efficiency in some semi-crystalline OPVs.

KEYWORDS: Bulk heterojunction solar cells, Organic photovoltaics, Monte Carlo simulation, geminate recombination, ternary blends, cascaded heterojunction

1. INTRODUCTION

Organic photovoltaic devices (OPVs) have the potential to be manufactured cheaply and scalably by either solution processing or evaporation. Since the introduction of the bulk heterojunction concept[1, 2], in which donor and acceptor materials are intermixed on a nanometer lengthscale in films ~100nm thick, the power conversion efficiency of OPVs has grown substantially and stands today in excess of 8% for solution-processed devices[3] and 10% for evaporated devices[4]. Yet this is still not sufficient for OPVs to have achieved widespread commercial use. A requirement of viable OPVs is that geminate charges formed by the dissociation of photo-generated excitons efficiently avoid recombination and be extracted at the electrodes. Separation of geminate charges in OPVs might be expected to be inefficient due to the small dielectric constant ($\varepsilon_r \approx$ 2-4) of molecular materials, which in turn leads to large Coulomb binding energies. This contrasts to competing inorganic technologies which have higher dielectric constants ($\varepsilon_r >$ 10) and show correspondingly efficient charge separation[5]. This challenge to OPVs has led researchers to take inspiration from photosynthesis where excited states are arranged in a 'cascade' that assists spatial separation of the electron and hole. This allows photosynthetic systems to achieve nearly unity charge separation efficiency[6-8], although this comes at significant cost in energy. This effect can be mimicked in OPVs by using three or more materials, that when used in conjunction, give a donor-cascade-acceptor heterojunction in which one charge is stabilized far from the heterojunction. Cascaded OPVs have been realized using evaporated small molecules[9-12], as well as solution-processed conjugated polymers blended with either fullerene derivatives[13-15] or carbon nanotubes[16, 17]. While these reports have shown OPV power conversion efficiency can be improved by cascaded heterojunctions, they have also shown that optimization is a laborious process that can result in mixed success.

Energy cascades may also affect the performance of OPVs beyond those with designed cascaded heterojunctions. Recent simulations suggest that energy cascades occur via self-organization in commonly studied poly(3-hexyl-thiophene) (P3HT):[6,6]-penyl-C61-butyric acid methyl ester (PCBM) OPVs[18]. In this case, P3HT chains adopt a more ordered structure, with a concomitantly smaller bandgap, further away from the PCBM interface. Since interfaces are more disordered between crystalline domains[19], this process may extend to other OPV systems where one component forms crystalline phases[18]. Energy cascades may therefore help explain why some OPV systems with components that crystallize have charge separation efficiencies, η_{GS} in excess of 60%[20, 21]. While it should be noted that good OPV performance can be achieved without crystallization (and presumably energy cascades)[22], the correlation between increased OPV performance and crystal formation in a number of systems[21] nonetheless invites further investigation into whether good charge separation efficiency is caused by the energy cascade formation.

This relates to an ongoing debate[23] as to why there is a gap between the reality of high performance in some, typically polymer-fullerene, OPVs and the expectations of poor performance due to the small dielectric constant in molecular systems. Indeed, some systems have been reported to be so efficient that η_{GS} is field independent[8]. For this to be the case there must be additional physics that causes the better-than-expected charge separation efficiency in some OPVs. A number of possible explanations have been proposed including charge delocalization[24, 25], dipoles[26] and energetic disorder[27, 28]. However, to-date, no studies have quantified how (possibly common) self-organized energy cascades affect charge separation.

Energy cascades are therefore of increasing interest because they offer the opportunity to design high performance ternary OPVs, and may help explain the high performance of binary OPVs in which one component crystallizes. In this Article a kinetic Monte Carlo model is used to examine the effect of a cascaded energy heterojunction upon geminate charge separation within OPVs. It is assumed that a 'cascade' material is interposed between the donor and acceptor as shown in **figure 1**. The energetic

characteristics of the cascade material are distinct from the donor and acceptor, whilst the thickness of the cascade material is also varied. This allowed examination of a wide range of designed ternary systems[9, 10, 12-14, 16, 17], in which the cascade material represents the third material, and self-organizing binary systems[18, 21], in which the cascade material represents the disordered boundary region between (crystallized) donor and acceptor. Using this model it is shown that energy cascades can lead to substantial improvements of η_{GS}, particularly at low electric fields. In particular, data for energy cascades similar to those reported for P3HT:PCBM self-organized heterojunctions show that η_{GS} is more than doubled at low fields compared to the case where the cascade is absent, and that the field dependence of η_{GS} is strongly reduced. However, these benefits depend sensitively upon the details of the energetic and positional structure of the cascade. It is shown that the heterostructure stops acting as a cascade beyond a cascade layer thickness of 3nm. These findings affirm the significant positive effects that cascaded energy heterojunctions can have upon OPV performance whilst underlining the importance of careful design of energy cascades.

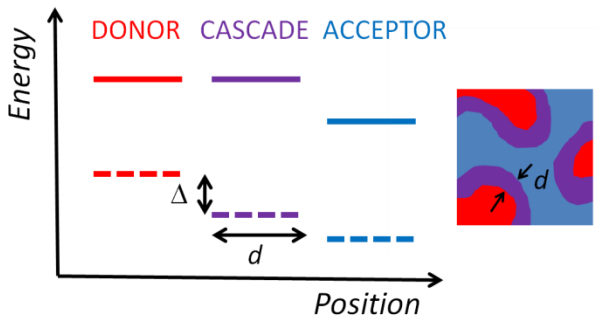

Figure 1. Schematic diagrams of band energies (left) and blend morphology (right) for a donor-cascade-acceptor heterojunction. Solid and dashed lines denote LUMO and HOMO levels respectively. Δ denotes the HOMO edge offset between donor and cascade material, and *d* is the thickness of the cascade layer separating donor and acceptor. The standard deviation of the Gaussian distributed density of states for the donor HOMO, cascade HOMO and acceptor LUMO are defined as σ_A, σ_C, and σ_D respectively.

2. MONTE CARLO SIMULATIONS

A Monte Carlo charge transport model similar to that reported elsewhere[29] was used to simulate η_{GS}. Models of this type have been shown to agree quantitatively with *J-V* curves of polymer bilayer OPV devices with abrupt[30] and roughened[31] interfaces. In the model, the OPV was represented as a 3D Cartesian array of hopping sites, each of size $1nm^3$, extending 128nm in each direction. Each site was initially defined as being either 'donor' or 'acceptor' conforming to either a bilayer morphology, in which the donor-acceptor interface was at the plane z = 64nm (z being parallel to the electric field), or a blend morphology, which had an optimized domain size of 7nm generated by a Cahn-Hilliard technique, post-processed to give sharp interfaces between donor and acceptor domains as well as pure domains (as used in reference 29). The initial donor-acceptor morphologies were then re-examined and all sites which were classified as donor and had an acceptor site within a radius d were re-assigned as 'cascade'. This interfacial cascade layer relates to the disordered region between two (more ordered) bulk phases in a binary OPV, while in a ternary OPV, the cascade layer represents the distinct material chosen to give the cascade effect.

The cascaded energy heterojunction shown in figure 1 was chosen to be similar to that of P3HT:PCBM[18]. This cascade is 'one-sided', *i.e.* only one charge (the hole) can make use of the cascade. Taking this diagram as a starting point, it was additionally assumed that electrons inhabit acceptor sites only, while holes inhabit either cascade or donor sites only. This assumes that the acceptor LUMO is always deep enough to accept electrons, while the cascade and donor HOMO is always shallow enough to accept holes. Energies for individual sites were chosen at random from Gaussian distributions to mimic the effects of energetic disorder. A Gaussian distribution is chosen since it is expected that this generally describes the distribution of HOMO and LUMO energies in conjugated polymers[32], although it should be noted that alternative distribution functions have been reported[33]. Practically this involves mapping random numbers between 0 and 1 to a Gaussian distribution using the Box-Muller transform. The

standard deviation of the acceptor LUMO, cascade HOMO and donor HOMO are denoted as σ_A, σ_C, and σ_D respectively. For all simulations it was assumed that $\sigma_A = \sigma_C = 100$meV, the large value of σ_C reflecting the expected conformational disorder in the transition between donor and acceptor materials[13]. Note that the values of energetic disorder were spatially uncorrelated.

A single charge separation simulation began with a geminate charge pair being injected at a randomly chosen cascade-acceptor interface. This means that charges were created with an energy distribution matching the density of states. Unless otherwise stated, charges were only allowed to hop to nearest-neighbor sites. In which case the hopping rate between the charge's current site *i* and allowed adjacent sites *j* was calculated using the following Marcus expression:

$$v_{i-j} = v_0 \exp\left\{-\frac{(E_j - E_i + E_r)^2}{4E_r kT}\right\}. \quad (1)$$

Here v_0 was 10^{11}s^{-1}, E_j and E_i are the site energies modified by electric field and Coulomb forces, the re-organization energy E_r = 0.25eV, k is Boltzmann's constant, and T = 298K was the temperature. The chosen parameters were similar to those used in other Monte Carlo models to describe charge transport in amorphous conjugated polymers[31]. Note that this approach implies a spatial averaging of the electronic coupling between molecules. This allows simulation of processes that occur over a large lengthscale (10s of nanometers), such as charge separation, but does not describe transport with the same degree of fidelity as is available in more complex quantum chemical calculations[34]. In some cases (noted in the text) variable range hopping was used. This involved multiplying the right hand side of equation (1) by $\exp\{-\alpha(r-1)\}$, where α = 5nm^{-1} was chosen as the localization radius of the electron and hole wavefunctions, and r is the hopping radius in nanometers. Coulomb forces between the charges were calculated assuming a dielectric constant of $\varepsilon = 3$. Recombination between adjacent charges was assumed to occur at a rate of $R_{rec} = 10^7$s^{-1}. It is noted that this recombination rate is the same as that used in a similar Monte Carlo model which obtained quantitative agreement with experimental *J-V* data for an

amorphous all-polymer OPV[30]. These parameters are expected to mimic the situation which occurs in amorphous all-polymer OPVs, in which field-activated η_{GS} has been reported[30, 31, 35]. This choice of parameters is deliberate since binary blends of amorphous materials are unlikely to form cascaded energy heterojunctions, therefore one can be reasonably confident that these parameters are free from the potential effects of energy cascades. Moreover, all-polymer OPVs show typically poor performance and so might be considered as an OPV system that could benefit from cascaded energy heterojunctions through a ternary architecture.

Particle behavior was determined by generating a waiting time for each possible process (*i.e.* hops, recombination events) using the following equation:

$$\tau = -\frac{ln(X)}{R}. \qquad (2)$$

Here X is a uniformly distributed random number between 0 and 1, while R is the rate of the process in question. Of all the possible events, the one with the shortest waiting time was selected as the behavior for that charge. When this was completed for both charges, time was advanced to the first event. If that event was a hop, the behavior of the charge was re-calculated once it was moved and re-inserted into the queue of events. Note that the behavior of the opposite charge was not re-calculated. This is the so-called first reaction method[36], which has been shown to be an effective method to reduce computer run-time without affecting the accuracy of OPV simulations[28]. Each single simulation was terminated when either the charges recombined, or if they achieved a separation of 25nm whereupon they were considered as having separated. A total of at least 7500 simulations were performed on 15 separate configurations of energetic disorder to ensure that the data presented is a representative average.

3. RESULTS AND DISCUSSION

Here the effect of individual parameters of the energy cascade, namely Δ, σ_D, and r, upon η_{GS} are examined. First the effect of the HOMO level shift, Δ is considered. **Figure 2a** and **2b** show predicted η_{GS} as a function of electric field for a bilayer and blend respectively for cascaded heterojunctions with $50meV \leq \Delta \leq 300meV$. These data assume $\sigma_D = \sigma_C = 100meV$ and $d = 1nm$. This is compared to data for an equivalent donor-acceptor heterojunction (i.e. $\Delta = 0$). Note that for a self-organized blend it would be expected that a reduction in bandgap (here related to an increase in HOMO shift, Δ as shown in **figure 1**) would be correlated with a reduction in energetic disorder, i.e. σ_D[18]. However, the aim here is to examine the effect of Δ independent of the other parameters, and so gradually build an understanding of how aspects of the cascade operate. For the donor-acceptor heterojunction (i.e. $\Delta = 0$) field-activated η_{GS} is shown, as expected, since polymer-like parameters were used. However, as the cascade is introduced by increasing Δ, η_{GS} increases substantially and becomes less field dependent. For $\Delta = 300meV$, η_{GS} is in excess of 0.92 and 0.87 for the bilayer and blend respectively over the entire investigated field range. This might be considered surprising given that the Coulomb binding energy for initially adjacent charge pairs in the investigated system is 480meV. However, to make the first hop away from the interface requires only 240meV (on average) so for a cascade with $\Delta = 300meV$ the first hop away from the interface is energetically favored and subsequent hops back to the interface are unlikely. Relating these data to OPVs, $\Delta = 300meV$ represents the upper end of reported HOMO level shifts between amorphous and crystalline P3HT[37, 38] which form the self-organized cascaded heterojunction in P3HT:PCBM OPVs[18]. There is, however, some uncertainty about the HOMO level shift between amorphous and crystalline P3HT since other reports have placed this value at 50meV[39] and 150meV[18]. It is noted that range separated Density Functional Theory (DFT) calculations can be used to calculate HOMO and LUMO levels from first principles[40-43], although these particular techniques have yet to be applied to the P3HT:PCBM which is the subject of discussion here. This approach would allow examination of the

effect of molecular packing on the HOMO level shift. Assuming a more moderate Δ = 150meV still results in significant improvements in η_{GS}, with low-field values of η_{GS} increasing by factors of more than 9 and 6 for the bilayer and blend respectively.

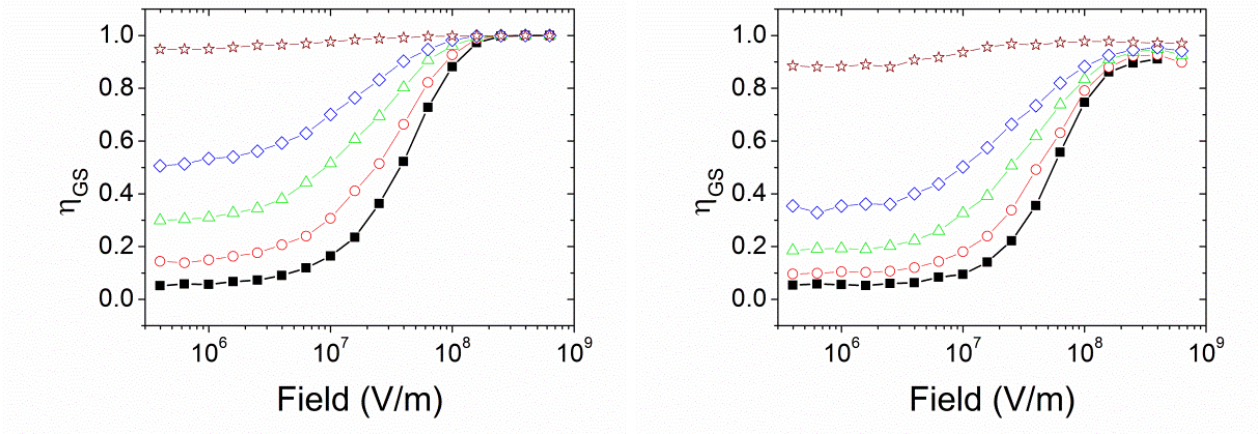

Figure 2. Charge separation efficiency, η_{GS}, as a function of electric field and HOMO band-edge offset, Δ for a bilayer (left) and a blend (right). Black filled squares denote a donor-acceptor heterojunction, while open symbols denote donor-cascade-acceptor heterojunctions with d = 1nm, σ_D = 100meV, and Δ = 50meV (red circles), 100meV (green triangles), 150meV (blue diamonds) and 300meV (purple stars).

More generally it can be seen that a HOMO level shift improves η_{GS} most significantly in the operating range of an OPV (10^6 - 10^7 V/m). This occurs for both the blend and bilayer, although η_{GS} in the blend improves less with HOMO level shift than in the bilayer. **Figure S1** in the **supplementary information** shows the factor improvement in η_{GS} between the cascaded and donor-acceptor heterojunction for the data shown in **figure 2**. It is proposed that the blend benefits less from the HOMO level shift because the hole must traverse a donor conducting network that is punctuated by cascade regions which pose an energetic barrier to long-range charge separation, which in turn arrests the process of charge separation. This is supported by measurements of the mean time to separation within the model which increased by a factor of more than 2 when cascaded heterojunctions are introduced to the blend

OPV. The difference in behavior between bilayer and blend morphologies was similar for all parameters considered, so hereafter only blend data are reported for brevity.

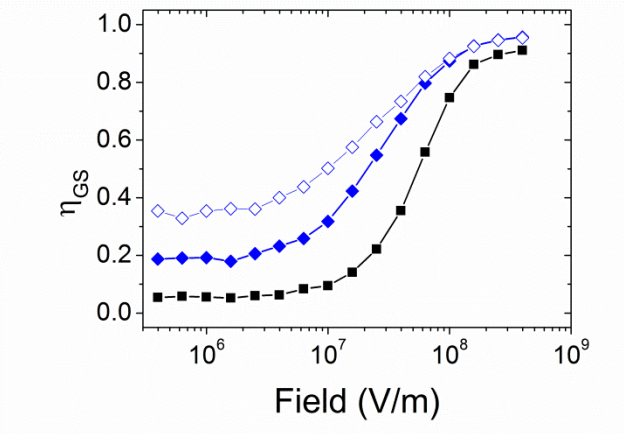

Figure 3. Charge separation efficiency, η_{GS}, as a function of electric field and σ_D in a blend. Diamonds denote a donor-cascade-acceptor heterojunction with d = 1nm and Δ = 150meV with (open) σ_D = 100meV and (closed) 50meV. Black filled squares denote a donor-acceptor heterojunction for comparison.

Since crystallization drives the self-organized cascaded systems and lowered energetic disorder is an expected consequence of crystallization[44], **figure 3** considers the effect a HOMO level shift, Δ, which is coupled with a reduction in the degree of energetic disorder in the donor, σ_D. Here it is assumed that d = 1nm and Δ = 150meV. It can be seen that η_{GS} reduces substantially when σ_D drops from 100meV to 50meV. Given that reduced energetic disorder leads to enhanced mobility, and increased mobility assists charge separation[45], it might be expected that η_{GS} would increase. However, as noted by Albrecht and Bässler[46] and others [27], relaxation within the density of states can assist charge separation. Reducing σ_D far from the donor-acceptor heterojunction reduces the efficacy of this process and so increases the degree of recombination, especially at small fields where the driving force for separation is small. This demonstrates that the different aspects of crystallization, i.e. changed bandgap[18, 37] and energetic

disorder[44], can have opposing effects. Indeed, if crystallization were not accompanied by a shift in the appropriate band-edge (the LUMO for the acceptor or HOMO for the donor), then crystallization is predicted to reduce OPV performance.

The data in **figures 2** and **3**, when taken together, suggest that trapping of charges far from an interface is beneficial to OPV performance. However, the converse picture to that examined here, in which charges are trapped *at* rather than *away from* an interface, has been shown to have a detrimental effect[45]. Hence the positioning of traps within the OPV is key to determining their eventual impact. Crystallization is a ready method by which energetic traps away from donor-acceptor interfaces can be formed. As already discussed, P3HT is expected to form hole traps at short distances away from P3HT:PCBM interfaces[18], but more generally, PCBM also forms aggregates/crystals with a higher electron affinity (~100meV) than finely intermixed PCBM[21]. This work therefore supports the suggestion that fullerene aggregation/crystallization may be one of the main reasons behind the success of polymer-fullerene devices[21]. It is worth noting that allied work has shown that charge trapping within a donor-acceptor bulk heterojunction morphology can substantially lower the rate of bimolecular recombination[47], in addition to geminate recombination as demonstrated here, and so crystallization may provide a double benefit. This is consistent with reports of crystallized P3HT:PCBM OPVs having inefficient geminate recombination[48] and an anomalously low rate of bimolecular recombination[49].

In **figure 4** the dependence of η_{GS} with width of cascade layer, *d* is plotted for Δ = 150meV (representing a mid-point in the range of reported Δ) and σ_D = 100meV. Self-organized P3HT:PCBM interfaces are predicted to transition between a disordered (high bandgap) state to a more ordered (low bandgap state) in ~3 P3HT monolayers from the P3HT:PCBM interface, while reported tri-layer devices have cascade layers with thicknesses up to several 10s of nanometers[9]. The effect of increasing *d* is profound, with the benefit of the cascade layer being reduced significantly for *d* = 3nm and almost removed completely for *d* = 10nm. This suggests that tri-layer devices having interposed layers with *d* >10nm[9] are in fact acting as back-to-back bilayers[50].

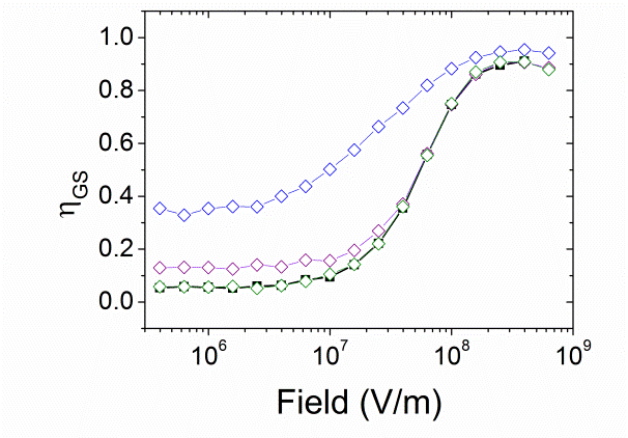

Figure 4. Charge separation efficiency, η_{GS}, as a function of electric field and *d* in a blend. Open symbols denote donor-cascade-acceptor heterojunctions with Δ = 150meV, σ_D = 100meV, and *d* = 1 (blue), 3 (purple) and 10nm (green). Black filled symbols denote a donor-acceptor heterojunction for comparison.

The reason for the strong *d* dependence of charge separation efficiency can be explained by the observation that geminate charges prior to recombination or separation typically have small separations due to mutual Coulomb interaction[51, 52]. Hence, the charge transport environment more than ~5nm distant from the donor-acceptor interface[51] is typically only explored by charges that are *en-route* to charge separation. Thus although a cascade can assist charge separation, the benefit is small when *d* is large since the charges affected were likely to separate anyway. This is in agreement with experiment, which shows that short circuit current is increased compared to the donor-acceptor equivalent when *d* = 2nm[12] and reduces therafter[9, 10, 12]. It should be noted that these data are not sensitive to the assumption of nearest-neighbor hopping, since the simulations were repeated allowing variable range hopping and quantitatively similar data were obtained, as shown in the **figure S2** of the **supplementary information**.

4. CONCLUSIONS

In this Article, the effect of cascaded energy heterojunctions, in which the spatial arrangement of energetic structure encourages charge separation, is examined using a kinetic Monte Carlo model. It is shown that cascaded energy heterojunctions with parameters similar to those reported in OPV devices do indeed lead to substantial improvements in charge separation efficiency. In some cases the improvement in performance was so profound that the separation efficiency became close to unity and field independent, perhaps offering an explanation as to why some OPV blends do not appear to suffer from recombination in spite of their low dielectic constant. This suggests that cascaded energy heterojunctions are an attractive route to design for high performance in OPV systems that otherwise would show low performance, e.g. all-polymer OPVs. Generally it is shown that cascades are at their most effective when they facilitate rapid charge transfer away from the interface (i.e. thin cascade layers) and subsequently trap them away from the counter charge (i.e. large HOMO/LUMO offsets and large disorder in the donor material). Increasing the distance charges have to traverse over the cascade reduces their effectiveness, turning the cascade into an unconnected series of junctions. It is hoped that the general efficacy of cascaded OPV structures demonstrated here will motivate further attempts to design cascaded OPVs, and quantum chemical studies examining the effect of cascades in specific systems.

ACKNOWLEDGEMENTS

The author thanks Alessandro Troisi and Richard Friend for useful discussions, and Nigel Clarke for use of the blend morphology. This work was carried out on Durham University's high performance computing cluster, *Hamilton*. The Monte Carlo code used to produce this work is copyright of the Cambridge University Enterprise and Durham University.

REFERENCES

1. G. Yu, J. Gao, J. C. Hummelen, F. Wudl and A. J. Heeger, *Science*, 1995, **270**, 1789-1791.
2. J. J. M. Halls, C. A. Walsh, N. C. Greenham, E. A. Marseglia, R. H. Friend, S. C. Moratti and A. B. Holmes, *Nature*, 1995, **376**, 498-500.
3. Polera Press Release, http://www.polyera.com/newsflash/world-record-inverted-opv-efficiency-acheived, Accessed 27th November 2012.
4. Heliatek Press Release, http://www.heliatek.com/wp-content/uploads/2012/09/120427_PI_Heliatek-world-record-10_7-percent-efficiency.pdf, Accessed 27th November 2012.
5. S. E. Gledhill, B. Scott and B. A. Gregg, *J. Mater. Res.*, 2005, **20**, 3167-3179.
6. H. Treutlein, K. Schulten, A. T. Bruger, M. Karplus, J. Deisenhofer and H. Michel, *Proc. Nat. Acad. Sci.*, 1992, **89**, 75-79.
7. D. A. LaVan and J. N. Cha, *Proc. Nat. Acad. Sci.*, 2006, **103**, 5251-5255.
8. T. M. Clarke and J. R. Durrant, *Chem. Rev.*, 2010, **110**, 6736-6767.
9. S. Sista, Y. Yao, Y. Yang, M. L. Tang and Z. A. Bao, *Appl. Phys. Lett.*, 2007, **91**, 223508.
10. Y. Kinoshita, T. Hasobe and H. Murata, *Appl. Phys. Lett.*, 2007, **91**, 083518.
11. C. W. Schlenker, V. S. Barlier, S. W. Chin, M. T. Whited, R. E. McAnally, S. R. Forrest and M. E. Thompson, *Chem. Mat.*, 2011, **23**, 4132-4140.
12. T. D. Heidel, D. Hochbaum, J. M. Sussman, V. Singh, M. E. Bahlke, I. Hiromi, J. Lee and M. A. Baldo, *J. Appl. Phys.*, 2011, **109**, 104502.
13. S. Honda, S. Yokoya, H. Ohkita, H. Benten and S. Ito, *J. Phys. Chem. C*, 2011, **115**, 11306-11317.
14. A. A. Bakulin, S. A. Zapunidy, M. S. Pshenichnikov, P. H. M. van Loosdrecht and D. Y. Paraschuk, *Phys. Chem. Chem. Phys.*, 2009, **11**, 7324-7330.
15. P. P. Khlyabich, B. Burkhart and B. C. Thompson, *J. Am. Chem. Soc.*, 2011, **134**, 9074-9077.
16. S. D. Stranks, C. Weisspfennig, P. Parkinson, M. B. Johnston, L. M. Herz and R. J. Nicholas, *Nano Lett.*, 2011, **11**, 66-72.
17. S. D. Stranks, C.-K. Yong, J. A. Alexander-Webber, C. Weisspfennig, M. B. Johnston, L. M. Herz and R. J. Nicholas, *ACS Nano*, 2012, **6**, 6058-6066.
18. D. P. McMahon, D. L. Cheung and A. Troisi, *J. Phys. Chem. Lett.*, 2011, **2**, 2737-2741.
19. P. G. De Gennes, *Scaling concepts in polymer physics*, Cornell University Press, Ithica, NY, 1985.
20. V. D. Mihailetchi, L. J. A. Koster, J. C. Hummelen and P. W. M. Blom, *Phys. Rev. Lett.*, 2004, **93**, 216601.
21. F. C. Jamieson, E. B. Domingo, T. McCarthy-Ward, M. Heeney, N. Stingelin and J. R. Durrant, *Chem. Sci.*, 2012, **3**, 485-492.
22. Y. Y. Liang, Z. Xu, J. B. Xia, S. T. Tsai, Y. Wu, G. Li, C. Ray and L. P. Yu, *Adv. Mater.*, 2010, **22**, E135-E138.
23. S. D. Baranovskii, M. Wiemer, A. V. Nenashev, F. Jansson and F. Gebhard, *J. Phys. Chem. Lett.*, 2012, **3**, 1214-1221.
24. C. Deibel, T. Strobel and V. Dyakonov, *Phys. Rev. Lett.*, 2009, **103**, 036402.
25. O. Rubel, S. D. Baranovskii, W. Stolz and F. Gebhard, *Phys. Rev. Lett.*, 2008, **100**, 196602.
26. V. I. Arkhipov, E. V. Emelianova and H. Bassler, *Phys. Rev. Lett.*, 1999, **82**, 1321-1324.
27. H. van Eersel, R. A. J. Janssen and M. Kemerink, *Adv. Funct. Mater.*, 2012, **22**, 2700-2708.
28. C. Groves, R. G. E. Kimber and A. B. Walker, *J. Chem. Phys.*, 2010, **133**, 144110.
29. B. P. Lyons, N. Clarke and C. Groves, *Energy Environ. Sci.*, 2012, **5**, 7657-7663.
30. R. G. E. Kimber, E. N. Wright, S. E. J. O'Kane, A. B. Walker and J. C. Blakesley, *Physical Review B (Condensed Matter and Materials Physics)*, 2013.
31. H. Yan, S. Swaraj, C. Wang, I. Hwang, N. C. Greenham, C. Groves, H. Ade and C. R. McNeill, *Adv. Funct. Mater.*, 2010, **20**, 4329-4337.
32. V. Coropceanu, J. Cornil, D. A. da Silva, Y. Olivier, R. Silbey and J. L. Bredas, *Chem. Rev.*, 2007, **107**, 926-952.
33. R. C. I. MacKenzie, C. C. Shuttle, M. L. Chablinyc and J. Nelson, *Adv. Energy Mater.*, 2012, **2**, 662-669.
34. J. L. Bredas, J. E. Norton, J. Cornil and V. Coropceanu, *Acc. Chem. Res.*, 2009, **42**, 1691-1699.
35. C. R. McNeill, S. Westenhoff, C. Groves, R. H. Friend and N. C. Greenham, *J. Phys. Chem. C*, 2007, **111**, 19153-19160.

36. J. J. Lukkien, J. P. L. Segers, P. A. J. Hilbers, R. J. Gelten and A. P. J. Jansen, *Phys. Rev. E*, 1998, **58**, 2598-2610.
37. W. C. Tsoi, S. J. Spencer, L. Yang, A. M. Ballantyne, P. G. Nicholson, A. Turnbull, A. G. Shard, C. E. Murphy, D. D. C. Bradley, J. Nelson and J.-S. Kim, *Macromolecules*, 2011, **44**, 2944-2952.
38. F. Paquin, G. Latini, M. Sakowicz, P.-L. Karsenti, L. Wang, D. Beljonne, N. Stingelin and C. Silva, *Phys. Rev. Lett.*, 2011, **106**, 197401.
39. T. M. Clarke, A. M. Ballantyne, J. Nelson, D. D. C. Bradley and J. R. Durrant, *Adv. Funct. Mater.*, 2008, **18**, 4029-4035.
40. B. M. Wong and T. H. Hsieh, *J. Chem. Theory Comput.*, 2010, **6**, 3704-3712.
41. T. Stein, H. Eisenberg, L. Kronik and R. Baer, *Phys. Rev. Lett.*, 2010, **105**, 4.
42. L. Kronik, T. Stein, S. Refaely-Abramson and R. Baer, *J. Chem. Theory Comput.*, 2012, **8**, 1515-1531.
43. M. E. Foster and B. M. Wong, *J. Chem. Theory Comput.*, 2012, **8**, 2682-2687.
44. R. J. Kline, M. D. McGehee, E. N. Kadnikova, J. Liu, J. M. J. Frechet and M. F. Toney, *Macromolecules*, 2005, **38**, 3312-3319.
45. C. Groves, J. C. Blakesley and N. C. Greenham, *Nano Lett.*, 2010, **10**, 1063-1069.
46. U. Albrecht and H. Bassler, *Chem. Phys. Lett.*, 1995, **235**, 389-393.
47. C. Groves and N. C. Greenham, *Phys. Rev. B*, 2008, **78**, 155205.
48. I. A. Howard, R. Mauer, M. Meister and F. Laquai, *J. Am. Chem. Soc.*, 2010, **132**, 14866-14876.
49. A. Pivrikas, N. S. Sariciftci, G. Juška and R. Österbacka, *Progress in Photovoltaics: Research and Applications*, 2007, **15**, 677-696.
50. K. Cnops, B. P. Rand, D. Cheyns and P. Heremans, *Appl. Phys. Lett.*, 2012, **101**, 143301.
51. C. Groves, R. A. Marsh and N. C. Greenham, *J. Chem. Phys.*, 2008, **129**, 114903.
52. R. G. E. Kimber, A. B. Walker, G. E. Schroder-Turk and D. J. Cleaver, *Phys. Chem. Chem. Phys.*, 2010, **12**, 844-851.